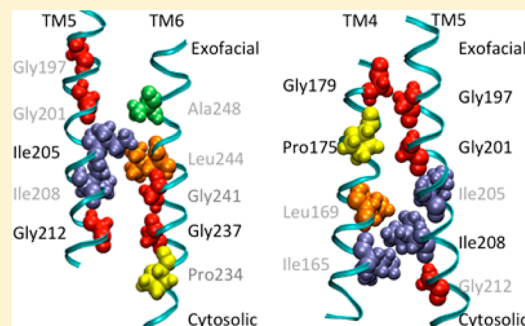


# Transmembrane Domain V Plays a Stabilizing Role in the Function of Human Bile Acid Transporter SLC10A2

Robyn H. Moore, Paresch Chothe, and Peter W. Swaan\*

Department of Pharmaceutical Sciences, University of Maryland, Baltimore, Maryland 21201, United States

**ABSTRACT:** The human apical sodium-dependent bile acid transporter (hASBT, SLC10A2), primarily expressed in the ileum, is involved in both the recycling of bile acids and cholesterol homeostasis. In this study, the structure–function relationship of transmembrane domain 5 (TM5) residues involved in transport is elucidated. Cysteine scanning mutagenesis of each consecutive residue on TM5 resulted in 96% of mutants having a significantly decreased transport activity, although each was expressed at the cell surface. Specifically, G197 and I208 were no longer functional, and G201 and G212 functioned at a level of <10% upon cysteine mutation. Interestingly, each of these exists along one face of the helix. Studies suggest that neither G201 nor G212 is on the substrate pathway. Conservative alanine mutations of the four residues displayed a higher activity in all but G197A, indicating its functional importance. G197 and G201 form a GxxxG motif, which has been found to be important in helix–helix interactions. According to our model, G197 and G201 face transmembrane domain 4 (TM4) residues G179 and P175, respectively. Similarly, G212 faces G237, which forms part of a GxxxG domain in transmembrane domain 6 (TM6). It is possible that these GxxxG domains and their interacting partners are responsible for maintaining the structure of the helices and their interactions with one another. I205 and I208 are both in positions to anchor the GxxxG domains and direct the change in interaction of TM5 from TM4 to TM6. Combined, the results suggest that residues along TM5 are critical for ASBT function but are not directly involved in substrate translocation.



The human apical sodium-dependent bile acid transporter (hASBT, SLC10A2), primarily expressed in the distal ileum, is involved in the recycling of bile acids. It is a highly efficient mechanism reclaiming 95% of the circulating bile acids daily.<sup>1</sup> ASBT is a 39–41 kDa active cotransporter of approximately one bile acid and two sodium ions per transport cycle.<sup>2</sup> As bile acids are synthesized *de novo* from cholesterol, ASBT is a potential drug target for lowering cholesterol levels in hypercholesterolemia.<sup>3–5</sup> Additionally, the efficiency of ASBT in transporting structurally diverse compounds makes it a target for a prodrug approach to improving drug bioavailability.<sup>6–10</sup> Currently, there is not a crystal structure of mammalian ASBT; therefore, a combination of molecular biology and computational techniques have been used by our laboratory to elucidate hASBT's structure–function relationships.

Previously, work from our lab has confirmed systematically that hASBT exhibits a seven-transmembrane (7TM) topology.<sup>11,12</sup> Further studies employed the use of cysteine scanning mutagenesis to identify structural requirements and interactions required for function. This method revealed that residues of TM6<sup>13</sup> and TM7<sup>14</sup> interact with bile acids on the exofacial half of the membrane while TM3<sup>15</sup> and TM4<sup>16</sup> interact with bile acids on the cytosolic half of the membrane. Combined, these data depict a substrate pathway through the membrane from its entrance to its release. Additionally, residues lining one face of TM6 may impart a helical flexibility required for the function of ASBT.<sup>13</sup> More recently, TM1 has

been shown to interact with sodium ions through several key residues.<sup>17</sup>

In this study, cysteine scanning mutagenesis and solvent accessibility studies of each consecutive residue in TM5 have been undertaken not only to understand the structure–function relationship of the residues involved in transport but also to elucidate how TM5 residues interact with nearby residues on adjacent TMs. TM5, similar to other TMs, is highly conserved among eukaryotic ASBT orthologs (Figure 1). Additionally, its proximity to TM4 and TM6 suggests a potential role is substrate translocation. TM5 could also interact with residues along TM6 to impart helical flexibility. In fact, the combination of results reported here indicates that TM5 plays primarily an indirect, structural role in the overall function of ASBT.

## EXPERIMENTAL PROCEDURES

**Materials.** [<sup>3</sup>H]Taurocholic acid (0.2 Ci/mmol) was purchased from PerkinElmer. Glycodeoxycholic acid (GDCA) and taurocholic acid (TCA) were purchased from Sigma. [2-(Trimethylammonium)ethyl] methanethiosulfonate bromide (MTSET) was purchased from Toronto Research Chemicals, Inc. Streptavidin Agarose Resin was purchased from Thermo

Received: January 8, 2013

Revised: June 26, 2013

Published: July 2, 2013



Human	191	KIILKIGSIAGAILVLIAVVGIL	215
Chimpanzee	191	KIILKIGSIAGAILVLIAVVGIL	215
Orangutan	154	KIILKIGSIAGAILVLIAVVGIL	178
Dog	191	KIILKVGSIAGAILVLIAVVGIL	215
Mouse	191	KIILKIGSITGVILVLIAVVGIL	215
Rat	202	KIILKIGSIAGAILVLIAVVGIL	226
Hamster	191	KIILKIGSIAGAILVLIAVVGIL	215
Rabbit	191	KIILKVGSIAGAILVLIAVVGIL	215
Pig	191	KIILKVGSIAGAILVLIAVVGIL	215
Zebrafish	191	KIILKVGSIAGAILVLIAVVGIL	215
		* **:* **:* **:* **:* **:	
<i>Neisseria meningitidis</i>	190	KLTDALPLVSVAAIVLIIAGAVVGAS	214
		* : : : : : *	

**Figure 1.** ASBT TMS sequence conservation across species. Sequences were aligned with ClustalW. Identical residues are denoted with asterisks; colons denote residues with a high degree of similarity, while periods denote weakly similar residues.

Scientific. Synthetic oligonucleotides were purchased from Sigma-Aldrich. Plasmids were prepared using a QIAprep Spin Mini-, Midi-, or Maxiprep kit from Qiagen. DNA sequencing was performed in the biopolymer laboratory at the University of Maryland (Baltimore, MD).

#### Site-Directed Mutagenesis and Protein Expression.

Cysteine and alanine point mutations were introduced on a hASBT C270A template in a pCMV5 vector because of the template's MTS insensitivity.<sup>18</sup> The mutations were generated by site-directed mutagenesis. The plasmids were sequenced, confirming the presence of each point mutation. Mutants were transiently transfected into COS-1 cells seeded at a density of  $6 \times 10^4$  cells/mL on a 24-well plate using the TurboFect Transfection Reagent from Thermo Scientific. Briefly, 0.5  $\mu$ g of plasmid DNA and 2  $\mu$ L of TurboFect Transfection Reagent per well were incubated for 15 min at room temperature in 100  $\mu$ L of DMEM. The mixture was then added to each well dropwise. Cells were used for further studies 24–48 h post-transfection. COS-1 cells were maintained as previously described.<sup>15</sup>

To determine the ASBT cell surface expression levels, biotinylation of the membrane proteins was conducted using a membrane impermeable EZ Link Sulfo-NHS-SS-Biotin reagent (Pierce) as described previously.<sup>19</sup> Briefly, cells were quickly washed twice with ice-cold PBS containing calcium and magnesium. The cells were incubated (500  $\mu$ L/well) with 1.2 mg/mL Sulfo-NHS-SS-Biotin for 30 min at 4 °C. The reaction was quenched with 300  $\mu$ L/well of 1 M Tris in PBS (pH 7.4). The cells were lysed in 300  $\mu$ L of NP-40 lysis buffer containing a protease cocktail per well and incubated for ~1 h at 4 °C while being rocked. A fraction of the lysate was removed for analysis as a total protein control. Soluble portions of the lysate were further treated with 250  $\mu$ L of Streptavidin Agarose Resin per well and incubated overnight at 4 °C on a nutator. The resin mixture was centrifuged for 1 min at 1000g, and the resin-attached proteins were incubated in 100  $\mu$ L of 2 $\times$  Laemmli buffer per well at room temperature for 40 min while being rocked. The samples were boiled for 10 min and stored at 4 °C. Western blotting was also performed as previously described.<sup>17</sup> Briefly, samples were loaded onto a precast, 15-well, 12% Tris-HCl polyacrylamide gel (Bio-Rad catalog no. 456-1046) along with 2.5  $\mu$ L of Li-cor Odyssey two-color protein molecular weight marker (catalog no. 928-40001). A custom antibody (1:1000) was used to visualize the glycosylated (41 kDa) and unglycosylated (38 kDa) hASBT protein. Additionally, the selective labeling of cell surface proteins was confirmed by the absence of the 90 kDa endoplasmic reticulum (ER) protein, calnexin (mouse anti-calnexin; 1:1000), and the presence of the

140 kDa cell surface protein pan-cadherin (mouse anti-cadherin; 1:1000).

**Uptake Assay and Sodium Activation.** TCA uptake experiments were conducted with slight modifications to previously reported methods.<sup>15,17</sup> Briefly, transiently transfected COS-1 cells were washed with warm Dulbecco's phosphate-buffered saline (DPBS) (pH 7.4) followed by equilibration in warm modified Hanks' balanced salt solution (MHBSS) (pH 7.4) at 37 °C for 15 min. Uptake was initiated by incubating cells in MHBSS containing 5.0  $\mu$ M TCA, 0.2% bovine serum albumin (BSA), and 1  $\mu$ Ci/mL [<sup>3</sup>H]TCA for 12 min at 37 °C. The reaction was halted when the cells were washed in ice-cold DPBS containing 0.5 mM TCA and 0.2% BSA. Liquid scintillation counting, using a LS6500 scintillation counter (Beckmann Coulter, Inc.), was used to measure the uptake of the cells after lysis in 350  $\mu$ L of 1 N NaOH. The total protein concentration was obtained by a Bradford assay to give a calculated rate of [<sup>3</sup>H]TCA internalization in picomoles per minute per milligram of protein. Normalization of the mutant to C270A was used as a means of comparison.

As described previously, the sensitivity of the mutants to sodium was determined by comparing the [<sup>3</sup>H]TCA transport function of the mutants at equilibrating (12 mM) and physiological (137 mM) sodium concentrations.<sup>15</sup> The uptake assay was conducted as described above but without the 15 min equilibration in MHBSS at 37 °C. Choline chloride was used to replace deficient sodium chloride. A ratio of 12 mM Na<sup>+</sup> uptake to 137 mM Na<sup>+</sup> uptake was calculated for each mutant and normalized to that of C270A.

**TCA and Sodium Kinetics.** TCA inhibition kinetics were determined for a select group of mutants using a range of TCA concentrations from 0 to 200  $\mu$ M, 137 mM NaCl, and 1  $\mu$ Ci/mL (0.2 Ci/mmol) [<sup>3</sup>H]TCA. Sodium kinetics were determined for sodium sensitive mutants using a range of sodium chloride concentrations from 0 to 200 mM, 5  $\mu$ M TCA, and 1  $\mu$ Ci/mL (0.2 Ci/mmol) [<sup>3</sup>H]TCA. Data were normalized to cell surface expression levels. Kinetic parameters were determined using GraphPad Prism version 5.0 as described previously.<sup>19</sup>

**MTSET Inhibition and Substrate Protection.** Transiently transfected COS-1 cells were incubated in 1 mM MTSET for 10 min at room temperature prior to being subjected to the uptake assay as described above.<sup>15,17,19</sup> Control cells, treated in MHBSS buffer alone, were run in parallel. The ratio of uptake for the MTSET-treated cells to the control cells was calculated to determine the inhibition of transport. This ratio was then compared to that of C270A. Additionally, as previously described, the transiently transfected cells were incubated in 1 mM MTSET with or without sodium and with or without 200  $\mu$ M GDCA for 10 min at room temperature prior to being subjected to the [<sup>3</sup>H]TCA uptake experiments as described above.<sup>15,17</sup> Again, ratios were calculated comparing each treatment to untreated (buffer only) cells, and these ratios were normalized to those of C270A.

**Data Analysis.** The data from each mutant are shown as the mean values with bars indicating the standard deviations (SDs) for  $n \geq 3$ . Data analysis was conducted using GraphPad Prism version 5.0 or Kaleidagraph version 4.0 using either a one-way analysis of variance (ANOVA) with a Dunnett's post hoc test or a two-tailed unpaired Student's *t* test as appropriate. Differences were considered statistically significant at  $p \leq 0.05$ .

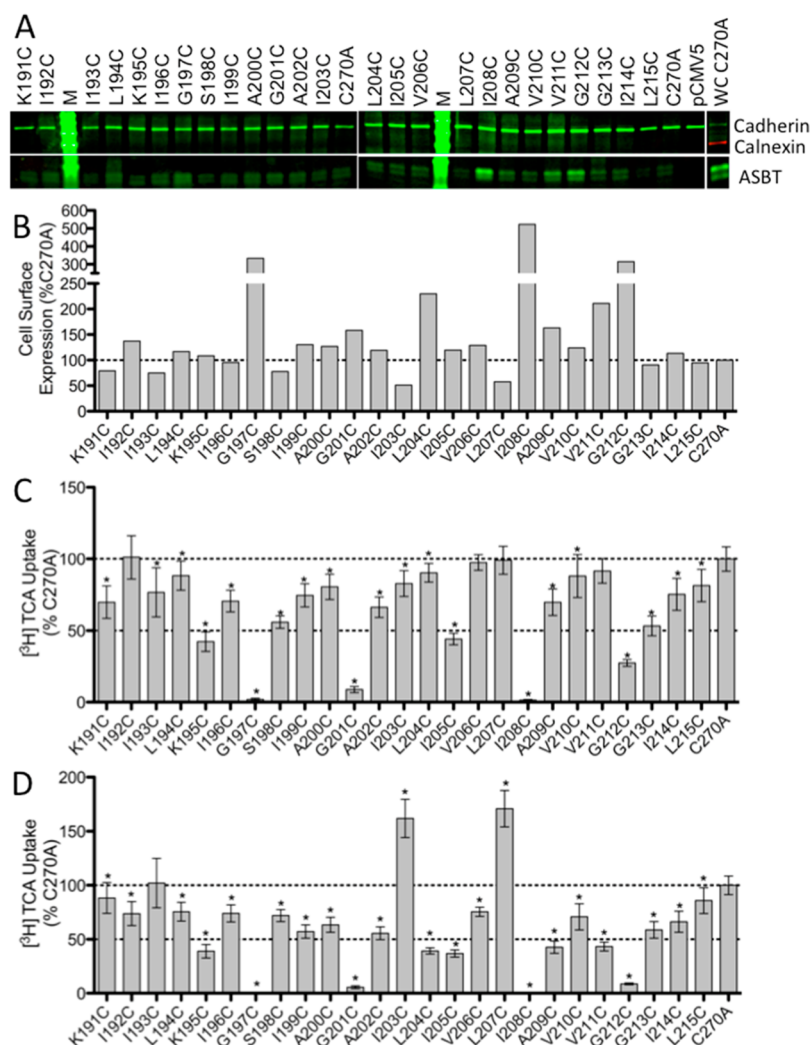


**Figure 2.** Protein expression and  $[^3\text{H}]\text{TCA}$  uptake in TM5 cysteine mutants. (A) Western blot of TM5 cysteine mutants expressed on the cell surface of COS-1 cells. ASBT is seen as two bands, glycosylated (41 kDa) and unglycosylated (38 kDa). Cadherin (140 kDa), expressed at the cell surface, was used as a positive loading control, while calnexin (90 kDa), expressed in the ER, was used as a negative control and was observed only in whole cell (WC) fractions (C270A is shown). Blots are representative of five independent experiments. (B) ASBT cell surface expression normalized to C270A. (C) Uptake of  $[^3\text{H}]\text{TCA}$  expressed as a percentage of the parental transporter, C270A, in picomoles of  $[^3\text{H}]\text{TCA}$  transported per minute per milligram of protein. (D) Uptake expressed as a percentage of C270A and normalized to ASBT cell surface expression. Bars represent the SD of at least three separate experiments performed in triplicate. A significant difference was determined by an ANOVA calculation with  $p < 0.05$  denoted with an asterisk.

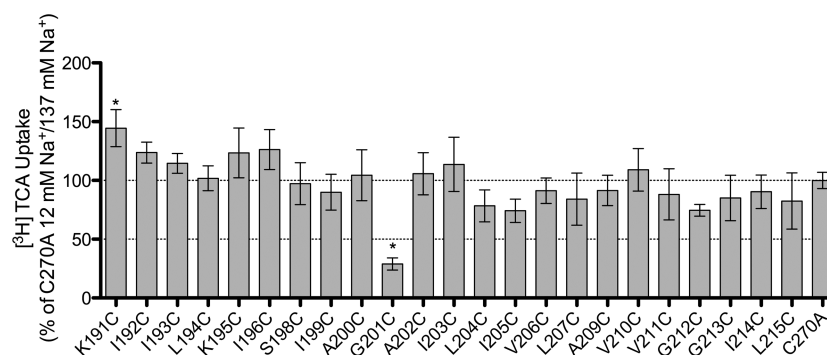


**Figure 3.** Sodium sensitivity of TM5 cysteine mutants. Uptake of  $[^3\text{H}]\text{TCA}$  in picomoles of  $[^3\text{H}]\text{TCA}$  transported per minute per milligram of protein. The graph represents a ratio of uptake at 12 and 137 mM sodium (1:1.84 for C270A) normalized as a percentage of the parental transporter, C270A. Bars represent the SDs of at least three separate experiments performed in triplicate. A significant difference was determined by an ANOVA calculation with  $p < 0.05$  denoted with an asterisk.



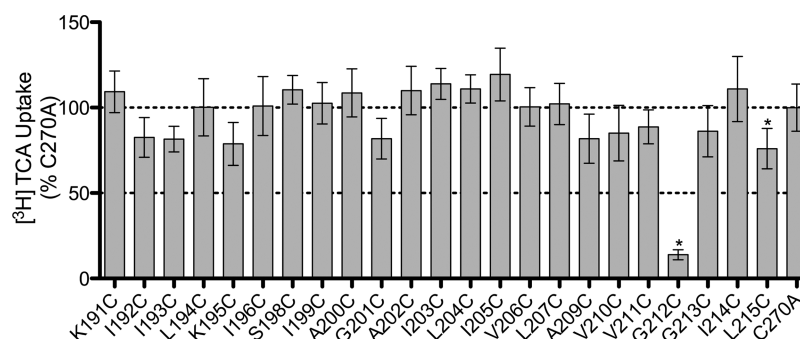


**Figure 4.** Identification of solvent accessible TMS mutant residues by MTSET labeling. Prior to [ $^3\text{H}$ ]TCA uptake, COS-1 cells expressing C270A or cysteine mutants were incubated with 1 mM MTSET for 10 min at room temperature. Uptake in the absence of MTSET was compared to uptake in the presence of MTSET (MTSET/initial) and represented as a percentage of that of C270A. Bars represent the SDs of at least three separate experiments performed in triplicate. A significant difference was determined by an ANOVA calculation with  $p < 0.05$  denoted with an asterisk.

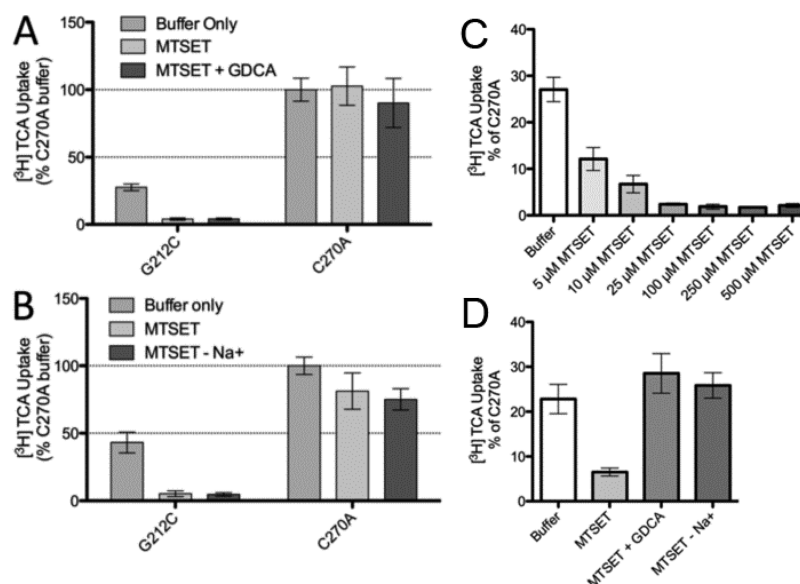


**Figure 5.** Protection of G212C from MTSET modification and MTSET does response. COS-1 cells expressing C270A or G212C were incubated with buffer alone or 1 mM MTSET (A) with or without GDCA or (B) with or without sodium for 10 min at room temperature. After being washed, cells were allowed to equilibrate to 37 °C for 15 min prior to [ $^3\text{H}$ ]TCA uptake. Each uptake was represented as a percentage of C270A uptake in buffer alone. Bars represent the SDs of at least three separate experiments performed in triplicate. A significant difference was determined by an ANOVA calculation with  $p < 0.05$  denoted with an asterisk. (C) COS-1 cells expressing G212C were incubated with buffer alone or 5–500  $\mu\text{M}$  MTSET for 10 min at room temperature. (D) COS-1 cells expressing G212C were incubated with buffer alone or 5  $\mu\text{M}$  MTSET with or without 200  $\mu\text{M}$  GDCA or with or without 137 mM sodium for 10 min at room temperature. After being washed, cells were allowed to equilibrate to 37 °C for 15 min prior to [ $^3\text{H}$ ]TCA uptake.

## RESULTS

**Membrane Expression and Uptake Activity of TM5 Cysteine Mutants.** Each residue along the TMS helix (Lys191–Leu215) was individually mutated to a cysteine residue in the C270A hASBT scaffold. The mutant DNA was then transiently transfected into COS-1 cells followed by studies of protein expression and function. Expression data indicate that each mutant generates protein that is present on the cell surface (Figure 2A).

After being normalized to membrane expression, results of activity assays of the cysteine mutants show that 88% of the mutants demonstrated a significant decrease in the rate of TCA uptake in comparison to that of C270A (Figure 2C). The activities for residues G197C and I208C were close to empty vector, pCMV5, indicating a near total loss of function. Additionally, G201C maintained only  $\sim 5.6\%$  of the activity of C270A, and G212C maintained approximately 8.8% of its

activity. The direct neighbors of each of these residues maintained at least 40% of the C270A activity.

**Sodium Activation.** Bile acid substrate is transported by ASBT through the use of the energy provided by the cotransport of sodium through a sodium gradient.<sup>2</sup> By altering the sodium concentration outside the cell from a physiological concentration (137 mM) to a concentration equal to that inside the cell, an equilibrating concentration (12 mM), and assaying the transport of TCA by the TM5 cysteine mutants, we were able to determine the involvement of the TM5 residues in sodium transport. Figure 3 shows the ratio of TCA transport for each mutant at 12 mM sodium versus 137 mM sodium in comparison to those of C270A. Only G201C shows a significant sensitivity to sodium in comparison to that of C270A.

**Substituted Cysteine Solvent Accessibility of TM5 Mutants.** Sulfhydryl groups of cysteine residues are predom-

**Table 1. Substrate Kinetics for Select TM5 Cysteine Mutants<sup>a</sup>**

	Na <sup>+</sup> kinetics		TCA kinetics	
	$J_{\max}$ [pmol min <sup>-1</sup> (mg of protein) <sup>-1</sup> ]	$K_{\text{Na}}$ (mM)	$J_{\max}$ [pmol min <sup>-1</sup> (mg of protein) <sup>-1</sup> ]	$K_{\text{TCA}}$ (μM)
C270A	249.1 ± 19.97	6.96 ± 2.36	1295 ± 131.6	9.60 ± 3.68
K191C <sup>b</sup>			1216 ± 113.3	7.32 ± 3.01
K195C <sup>b</sup>			360.7 ± 44.22 <sup>e</sup>	3.91 ± 2.77
G201C <sup>b,c</sup>	30.25 ± 2.34 <sup>e</sup>	31.08 ± 6.84 <sup>e</sup>	140.4 ± 17.85 <sup>e</sup>	4.64 ± 3.14
I205C <sup>b</sup>			950.0 ± 86.36 <sup>e</sup>	5.32 ± 2.42
G212C <sup>b,d</sup>			199.4 ± 27.21 <sup>e</sup>	11.49 ± 5.86

<sup>a</sup>Sodium concentrations ranged from 0 to 200 mM (5 μM TCA) and TCA concentrations from 0 to 200 μM (137 mM Na<sup>+</sup>). Data, with standard errors, represent at least three separate experiments performed in triplicate. Kinetic parameters were determined using GraphPad Prism version 5.0, with constants determined by nonlinear regression. Parameters determined to be significant compared to those of the C270A control ± SD when analyzed by one-way ANOVA (TCA kinetics) or *t* test (Na<sup>+</sup> kinetics) are indicated. <sup>b</sup>Decreased uptake upon cysteine mutation. <sup>c</sup>Sodium sensitive. <sup>d</sup>MTSET accessible. <sup>e</sup>*p* ≤ 0.05.

inantly deprotonated in aqueous environments, allowing for a facile reaction with MTSET, which reacts selectively with ionized sulfhydryl groups.<sup>20–22</sup> Using this chemistry as an advantage, the MTSET reagent can be incubated with the cysteine mutants; then, the chemically modified mutants can be assayed for transport function to identify residues that are in aqueous environments. In the TMs, these environments could signify a substrate pathway or a binding pocket. The TM5 data demonstrate a highly significant decrease in transport activity after MTSET treatment for G212C only (Figure 4).

**Substrate Protection of G212C.** Substrate protection of mutants in the presence of MTSET can occur under two conditions; the substrate can interact directly with the mutant residue and inhibit an interaction with MTSET, or it can interact at a site away from the residue, causing a change in the conformation of the protein and inhibiting the access of MTSET. To determine if ASBT substrates interact with G212C in the presence of MTSET, buffers containing GDCA or lacking Na<sup>+</sup> were co-incubated with MTSET prior to the transport assay. In the case of both GDCA and Na<sup>+</sup>, the presence of substrate was not able to rescue the transport function of the mutant (Figure 5A,B). These results indicate that G212C is solvent accessible in the presence or absence of substrate and can be modified by MTSET under both conditions. Therefore, it is likely that the interaction between G212C and MTSET alone is altering the activity of the mutant protein and that neither bile acid nor sodium is directly or indirectly interacting with G212C to alter its accessibility. Additionally, we validated the dose response of MTSET (5–500 μM) to determine whether G212C is highly sensitive to inhibition by MTSET (Figure 5C). At low MTSET concentrations (5–10 μM), the extent of functional inhibition was reduced (apparent IC<sub>50</sub> of 4.1 μM), and subsequent experiments at 5 μM MTSET (Figure 5D) revealed that substrate (GDCA) and the presence of Na<sup>+</sup> were both able to rescue ASBT from MTSET inactivation. These data suggest that conformational changes may occur in the presence of bile acid and sodium that protects this residue from modification; this effect may be reversed by increasing MTSET concentrations.

**TCA and Sodium Kinetics of TM5 Mutants.** Kinetic analysis was performed on select TM5 mutants in an attempt to further understand their roles. TCA affinity ( $K_{\text{TCA}}$ ) was not significantly altered in any of the five mutants tested (Table 1). However,  $J_{\max}$  was significantly lower in four of the five mutants tested. Additionally, a significant decrease in the affinity for

sodium ( $K_{\text{Na}}$ ) as well as a significant decrease in  $J_{\max}$  was also observed for G201C.

**Select Conservative Mutations in TM5.** The results described above, suggesting that neither TCA nor sodium is being directly transported by the residues in TM5, prompted a further investigation into the structural relevance of the residues exhibiting decreased activity. Residues displaying a complete or nearly complete loss of activity due to cysteine mutation (G197C, G201C, I208C, and G212C) were mutated to the more conservative alanine in the C270A background. Alanine mutants were assessed for function by a [<sup>3</sup>H]TCA uptake assay (Figure 6). While G197A remained inactive and the activity of G201A remained relatively similar to that of G201C, the activities of I208A and G212A increased significantly from those of their cysteine counterparts. The sodium sensitivities of G201A and I208A were also determined (Figure 6B). While G201A remains sodium sensitive, I208A was found to be insensitive to sodium. These results support earlier data suggesting that, other than G201, TM5 does not play a role in sodium transport and that G201 may be indirectly involved.

## DISCUSSION

hASBT, primarily expressed in the distal ileum, is involved in the recycling of bile acids and is critical for cholesterol homeostasis. Given its biological importance and its potential role in drug transport, characterization at the functional and structural level would allow rational drug design for ASBT as a pharmacological target. Previous studies in our lab have elucidated roles for several TMs and extracellular loops in ASBT.<sup>12–17,19,23</sup> For example, TM3 and TM4 have been shown to play a role in TCA translocation on the cytosolic half of the protein.<sup>15,16</sup> In the study presented here, the structure–function relationship of the TM5 residues involved in transport has been revealed. While TM5 residues may not play a direct role in the transport of either bile acids or sodium, several appear to play a critical role in α-helical stability.

The alignment of TM5 residues from humans with those of nine eukaryotic orthologs demonstrates a highly conserved sequence with 22 of the 25 residues being either identical or highly similar (Figure 1). As expected, cysteine scanning mutagenesis of these residues indicated that the majority of residues, 96%, were sensitive to cysteine mutation (Figure 2). However, most mutants maintained more than 35% activity. Of the remaining evolutionarily conserved, low-activity residues, the activity of G201C (5.6%) and G212C (8.8%) was severely hampered by cysteine substitution while mutants G197C and I208C had a total loss of function. Interestingly, all four

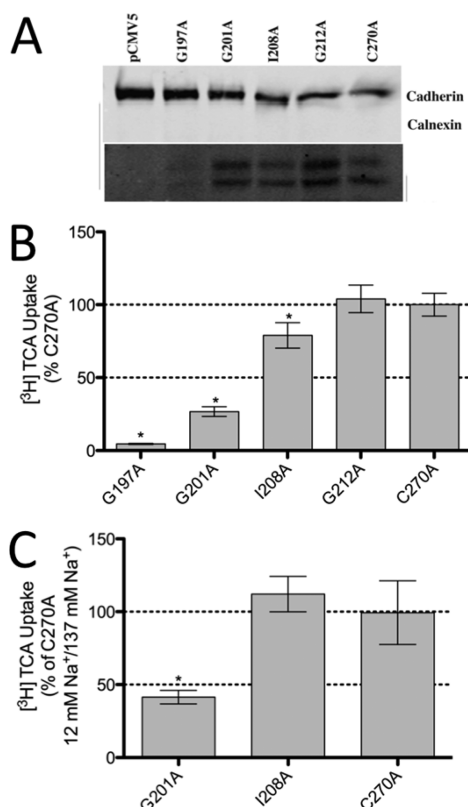


**Figure 6.**  $[^3\text{H}]\text{TCA}$  uptake and sodium sensitivity of select TMS alanine mutants. (A) Western blot of TMS alanine mutants expressed on the cell surface of COS-1 cells. ASBT is seen as two bands. Cadherin (140 kDa), expressed at the cell surface, was used as a positive loading control, while calnexin (90 kDa), expressed in the ER, was used as a negative control. (B) Uptake of  $[^3\text{H}]\text{TCA}$  expressed as a percentage of the parental transporter, C270A, in picomoles of  $[^3\text{H}]\text{TCA}$  transported per minute per milligram of protein. (C) Uptake of  $[^3\text{H}]\text{TCA}$  in picomoles of  $[^3\text{H}]\text{TCA}$  transported per minute per milligram of protein. The graph represents a ratio of uptake at 12 mM sodium to 137 mM sodium normalized as a percentage of the parental transporter, C270A. Bars represent the SDs of at least three separate experiments performed in triplicate. A significant difference was determined by an ANOVA calculation with  $p < 0.05$  denoted with an asterisk.

residues reside on the same face of the helix (Figure 7A).<sup>12</sup> Upon alanine mutation, G197A remained inactive; however, the activity of the other residues was restored partially (G201A, 27%) or completely (I208A and G212A) (Figure 6). While it is possible that the mutation of these glycine residues alone could disrupt the helical structure in TMS, the high concentration of functionally relevant glycines on one face of the helix warranted additional investigation.

To determine the TMS mutants' sensitivity to sodium, the effect of TCA transport was determined at equilibrative sodium concentrations and compared to those at physiological concentrations. One residue, G201C, was found to be sensitive to sodium concentrations (Figure 3). The sensitivity to sodium was reproduced in the G201A mutant (Figure 6B). Kinetic studies of G201C revealed a significant decrease in sodium affinity (Table 1). These results indicate a role for G201 in sodium transport, but it is unlikely to be a direct interaction as other TMS residues are not involved (*vide infra*).

The identification of solvent accessible residues can reveal a substrate translocation pathway. We applied the substituted

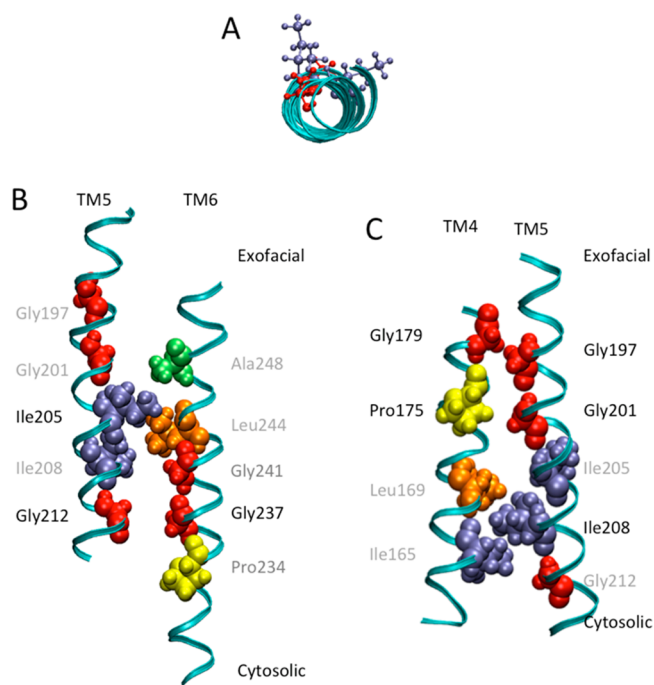


**Figure 7.** *In silico* representation of TMS residues relevant for ASBT function. (A) Top down view of TMS from the exofacial side of the membrane highlighting relevant amino acids residing on the same face of the helix. Ball-and-stick representations colored red denote glycine residues, while purple denotes isoleucine residues. (B) *In silico* prediction of TMS and TM6 functional group orientation. The GxxxG motif of TM6 (Gly237 and Gly241) potentially associates with Gly212 of TMS at the backbone level to stabilize the helices. Ile205 may participate to constrain the crossing angle of the two helices. (C) *In silico* prediction of TM4 and TM5 functional group orientation. The GxxxG motif in TMS (Gly197 and Gly201) potentially interacts with Gly179 and Pro175, respectively, to allow for a strong and close association of the two helices. Ile208 interacts with Ile165 and Leu169 to anchor and constrain the crossing angles of the helices. Images were generated with VMD version 1.8.6.

cysteine accessibility method (SCAM) by incubating each mutant, expressed in COS-1 cells, with the membrane impermeable MTSET reagent prior to uptake studies (Figure 4). This study pointed to only one solvent accessible residue, G212C. Additionally, TCA kinetic data on this residue indicated a slight decrease in substrate affinity in comparison to that of the C270A control (Table 1). In an attempt to modify the accessibility of this residue to MTSET, experiments were conducted either in the presence of GDCA or in the absence of sodium (Figure 5). As observed previously with the wild type (WT) and other TM mutants, substrate protection can partially or fully restore protein activity to levels seen when uptake is conducted in buffer alone. Co-incubation of MTSET with GDCA or in the absence of sodium did not alter the solvent accessibility, suggesting that neither substrate is directly interacting with G212 and that conformational changes that would inhibit MTSET from accessing the residue are not occurring. Therefore, while G212C is solvent accessible, it does not appear to be in the substrate or cosubstrate pathway.

A new dimer model (manuscript submitted) shows that G212 lies near the proposed, solvent accessible, dimer interface.<sup>24</sup> The interface is formed among the TM1, TM7, and TM6 regions. TMS is close to TM6 of the same monomer and next to TM1 of the other monomer in the hASBT dimer.



Because TM5 is in the proximity of the water accessible interface, it is possible that G212 is affected by MTSET through this pathway.

Glycine and proline residues are known to destabilize and impart flexibility upon  $\alpha$ -helices.<sup>25</sup> This increase in flexibility is important in transmembrane proteins that do not usually possess much inherent flexibility within the membrane but require conformational changes during turnover.<sup>26</sup> Alternatively, these glycine residues may be involved in the stabilization of the helix. The loss of flexibility due to the mutation of the glycine residues in TM5 to cysteines or even to alanines could, in part, explain the decrease in or loss of activity observed. The GxxxG motif is commonly found in  $\alpha$ -helices of transmembrane proteins<sup>25,27–33</sup> and has been found to be important in the association of two adjacent TMs. The small size of the glycine residues on the same face of the helix allows for the proximity of the two interacting helices so that the backbone structure of the helix can interact, either through hydrogen bonding or through van der Waals forces, with the backbone of the adjacent helix.<sup>27,28,31</sup>

According to our validated structural model of hASBT, Gly212, on the cytosolic side of the membrane, is facing TM6 residue Gly237 that is part of the Pro234/Gly237/Gly241 conformational switch (Figure 7B).<sup>13</sup> The presence of the GxxxG motif in the conformational switch and its interaction with Gly212 could explain why the mutation of Gly212 to cysteine resulted in impaired function. It is possible that the mutation of Gly212 to alanine resulted in a fully functional transporter because the small size of the alanine could still allow for the required interactions between helices. Another possibility is that Gly213 was able to moderately compensate for the loss of Gly212. On the exofacial side of the membrane, Gly197 and Gly201 of TM5 are facing TM4 residues Gly179 and Pro175, respectively (Figure 7C). Like Gly197, Gly179 also has a total loss of function when mutated to cysteine.<sup>16</sup> Additionally, both G201 and P175 are sodium sensitive. In the case of Gly197, it is possible that the alanine mutation was sufficient to disrupt the packing of the helices that resulted in a total loss of function. However, it seems clear that these helix–helix associations are likely responsible for the stability of the helices and thus the GxxxG motifs and their interacting residues are required for function. Further, while it is possible that sodium could interact with the backbone residues of G201, it is more likely that G201 plays a role in the helix–helix interaction and that its role in sodium transport is indirect. The sodium sensitivity of G201 mutants may be attributed to conformational changes caused by the disruption of the helical interactions.

Recently, a crystal structure of an ASBT ortholog from *Neisseria meningitidis* (Asbt<sub>NM</sub>) was reported,<sup>34</sup> with a sequence 26% identical to that of hASBT. Asbt<sub>NM</sub> was found to contain 10 TM domains,<sup>34</sup> differing from the verified seven-TM topology model of hASBT.<sup>11,12</sup> TM7 of Asbt<sub>NM</sub> coincides with TM5 in hASBT and is 12% identical when aligned with the 10 eukaryotic species seen in Figure 1. TM7 of Asbt<sub>NM</sub> transects the membrane from the cytosolic side of the membrane to the exofacial side, while TM5 of hASBT transects the membrane in the opposite direction. Additionally, the crystal structure indicates that the residues of TM7 in Asbt<sub>NM</sub> corresponding to the functionally significant residues of TM5 in hASBT, interact with the nonconserved TM1. In hASBT, Asn10 in the N-terminal segment is glycosylated, and therefore, the N-terminal segment does not reside within the membrane

as it does in Asbt<sub>NM</sub>. The many differences in topology and sequence identity could be due to many factors, including the evolutionary distance and the differences in membrane composition. Also, as the native substrate for Asbt<sub>NM</sub> has not been identified, substrate affinity differences could contribute to the diversity of topology and sequence identity. At this point, it remains unclear whether the structure of Asbt<sub>NM</sub> has any correlation with or relevance to that of hASBT, but further investigation into the structure–function relationship between residues in Asbt<sub>NM</sub> may provide more insight.

Overall, data suggest that residues along one face of TM5 do not play a direct role in substrate transport but are critical for ASBT function, most likely through helical stability. The GxxxG motifs and their interacting residues along TM4–TM6 potentially allow for a close association of the helices at various positions, by serving as scaffolds for the other portions of the helices to interact with substrate. Additionally, I205 and I208 may constrain the crossing angles of TM5 and the other helices and may direct the change in interaction of TM5 from TM4 to TM6. This further insight into the structure–function relationship of ASBT may aid in future studies involving drug or prodrug design for the treatment of various diseases.

## AUTHOR INFORMATION

### Corresponding Author

\*Department of Pharmaceutical Sciences, University of Maryland, 20 Penn St., Baltimore, MD 21201. E-mail: pswaan@rx.umaryland.edu. Telephone: (410) 706-0103. Fax: (410) 706-5017.

### Funding

This research was supported by a grant from the National Institutes of Health, National Institute for Diabetes and Digestive and Kidney Diseases Grant DK061425 to P.W.S.

### Notes

The authors declare no competing financial interest.

## ACKNOWLEDGMENTS

We thank Dr. Tatiana Claro da Silva for her technical guidance and support. We also thank Dr. Sairam Mallajosyula for assistance with modeling and VMD.

## ABBREVIATIONS

GDCA, glycodeoxycholic acid; hASBT, human apical sodium-dependent bile acid transporter; MTSET, [2-(trimethylammonium)ethyl] methanethiosulfonate; SCAM, substituted cysteine accessibility method; TCA, taurocholic acid; TM, transmembrane domain.

## REFERENCES

- (1) Dawson, P. A., Lan, T., and Rao, A. (2009) Bile acid transporters. *J. Lipid Res.* 50, 2340–2357.
- (2) Weinman, S. A., Carruth, M. W., and Dawson, P. A. (1998) Bile acid uptake via the human apical sodium-bile acid cotransporter is electrogenic. *J. Biol. Chem.* 273, 34691–34695.
- (3) Izzat, N. N., Deshazer, M. E., and Loose-Mitchell, D. S. (2000) New molecular targets for cholesterol-lowering therapy. *J. Pharmacol. Exp. Ther.* 293, 315–320.
- (4) Kitayama, K., Nakai, D., Kono, K., van der Hoop, A. G., Kurata, H., de Wit, E. C., Cohen, L. H., Inaba, T., and Kohama, T. (2006) Novel non-systemic inhibitor of ileal apical Na<sup>+</sup>-dependent bile acid transporter reduces serum cholesterol levels in hamsters and monkeys. *Eur. J. Pharmacol.* 539, 89–98.

- (5) Kramer, W., and Glombik, H. (2006) Bile acid reabsorption inhibitors (BARI): Novel hypolipidemic drugs. *Curr. Med. Chem.* 13, 997–1016.
- (6) Balakrishnan, A., and Polli, J. E. (2006) Apical sodium dependent bile acid transporter (ASBT, SLC10A2): A potential prodrug target. *Mol. Pharmaceutics* 3, 223–230.
- (7) Balakrishnan, A., Wring, S. A., and Polli, J. E. (2006) Interaction of native bile acids with human apical sodium-dependent bile acid transporter (hASBT): Influence of steroidal hydroxylation pattern and C-24 conjugation. *Pharm. Res.* 23, 1451–1459.
- (8) Kagedahl, M., Swaan, P. W., Redemann, C. T., Tang, M., Craik, C. S., Szoka, F. C., Jr., and Oie, S. (1997) Use of the intestinal bile acid transporter for the uptake of cholic acid conjugates with HIV-1 protease inhibitory activity. *Pharm. Res.* 14, 176–180.
- (9) Swaan, P. W., Hillgren, K. M., Szoka, F. C., Jr., and Oie, S. (1997) Enhanced transepithelial transport of peptides by conjugation to cholic acid. *Bioconjugate Chem.* 8, 520–525.
- (10) Tolle-Sander, S., Lentz, K. A., Maeda, D. Y., Coop, A., and Polli, J. E. (2004) Increased acyclovir oral bioavailability via a bile acid conjugate. *Mol. Pharmaceutics* 1, 40–48.
- (11) Banerjee, A., and Swaan, P. W. (2006) Membrane topology of human ASBT (SLC10A2) determined by dual label epitope insertion scanning mutagenesis. New evidence for seven transmembrane domains. *Biochemistry* 45, 943–953.
- (12) Zhang, E. Y., Phelps, M. A., Banerjee, A., Khantwal, C. M., Chang, C., Helsper, F., and Swaan, P. W. (2004) Topology scanning and putative three-dimensional structure of the extracellular binding domains of the apical sodium-dependent bile acid transporter (SLC10A2). *Biochemistry* 43, 11380–11392.
- (13) Hussainzada, N., Khandewal, A., and Swaan, P. W. (2008) Conformational flexibility of helix VI is essential for substrate permeation of the human apical sodium-dependent bile acid transporter. *Mol. Pharmacol.* 73, 305–313.
- (14) Hussainzada, N., Banerjee, A., and Swaan, P. W. (2006) Transmembrane domain VII of the human apical sodium-dependent bile acid transporter ASBT (SLC10A2) lines the substrate translocation pathway. *Mol. Pharmacol.* 70, 1565–1574.
- (15) Hussainzada, N., Claro Da Silva, T., and Swaan, P. W. (2009) The cytosolic half of helix III forms the substrate exit route during permeation events of the sodium/bile acid cotransporter ASBT. *Biochemistry* 48, 8528–8539.
- (16) Khantwal, C. M., and Swaan, P. W. (2008) Cytosolic half of transmembrane domain IV of the human bile acid transporter hASBT (SLC10A2) forms part of the substrate translocation pathway. *Biochemistry* 47, 3606–3614.
- (17) Claro da Silva, T., Hussainzada, N., Khantwal, C. M., Polli, J. E., and Swaan, P. W. (2011) Transmembrane helix 1 contributes to substrate translocation and protein stability of bile acid transporter SLC10A2. *J. Biol. Chem.* 286, 27322–27332.
- (18) Banerjee, A., Ray, A., Chang, C., and Swaan, P. W. (2005) Site-directed mutagenesis and use of bile acid-MTS conjugates to probe the role of cysteines in the human apical sodium-dependent bile acid transporter (SLC10A2). *Biochemistry* 44, 8908–8917.
- (19) Hussainzada, N., Da Silva, T. C., Zhang, E. Y., and Swaan, P. W. (2008) Conserved aspartic acid residues lining the extracellular loop 1 of sodium-coupled bile acid transporter ASBT Interact with Na<sup>+</sup> and 7 $\alpha$ -OH moieties on the ligand cholestane skeleton. *J. Biol. Chem.* 283, 20653–20663.
- (20) Absalom, N. L., Schofield, P. R., and Lewis, T. M. (2009) Pore structure of the Cys-loop ligand-gated ion channels. *Neurochem. Res.* 34, 1805–1815.
- (21) Karlin, A., and Akabas, M. H. (1998) Substituted-cysteine accessibility method. *Methods Enzymol.* 293, 123–145.
- (22) Ray, A., Banerjee, A., Chang, C., Khantwal, C. M., and Swaan, P. W. (2006) Design of novel synthetic MTS conjugates of bile acids for site-directed sulfhydryl labeling of cysteine residues in bile acid binding and transporting proteins. *Bioorg. Med. Chem. Lett.* 16, 1473–1476.
- (23) Banerjee, A., Hussainzada, N., Khandewal, A., and Swaan, P. W. (2008) Electrostatic and potential cation- $\pi$  forces may guide the interaction of extracellular loop III with Na<sup>+</sup> and bile acids for human apical Na<sup>+</sup>-dependent bile acid transporter. *Biochem. J.* 410, 391–400.
- (24) Mallajosyula, S. S., Sabit, H., Swaan, P. W., MacKerell, J., and Alexander, D. (2013) Human Bile Acid Transporter (hASBT) Functions as a Dimer. Manuscript submitted for publication.
- (25) Javadpour, M. M., Eilers, M., Groesbeek, M., and Smith, S. O. (1999) Helix packing in polytopic membrane proteins: Role of glycine in transmembrane helix association. *Biophys. J.* 77, 1609–1618.
- (26) Kaback, H. R., and Wu, J. (1997) From membrane to molecule to the third amino acid from the left with a membrane transport protein. *Q. Rev. Biophys.* 30, 333–364.
- (27) Kleiger, G., and Eisenberg, D. (2002) GXXXG and GXXXA motifs stabilize FAD and NAD(P)-binding Rossmann folds through C( $\alpha$ )-H $\cdots$ O hydrogen bonds and van der Waals interactions. *J. Mol. Biol.* 323, 69–76.
- (28) MacKenzie, K. R., Prestegard, J. H., and Engelman, D. M. (1997) A transmembrane helix dimer: Structure and implications. *Science* 276, 131–133.
- (29) Schneider, D., and Engelman, D. M. (2004) Motifs of two small residues can assist but are not sufficient to mediate transmembrane helix interactions. *J. Mol. Biol.* 343, 799–804.
- (30) Senes, A., Engel, D. E., and DeGrado, W. F. (2004) Folding of helical membrane proteins: The role of polar, GxxxG-like and proline motifs. *Curr. Opin. Struct. Biol.* 14, 465–479.
- (31) Eilers, M., Patel, A. B., Liu, W., and Smith, S. O. (2002) Comparison of helix interactions in membrane and soluble  $\alpha$ -bundle proteins. *Biophys. J.* 82, 2720–2736.
- (32) Curran, A. R., and Engelman, D. M. (2003) Sequence motifs, polar interactions and conformational changes in helical membrane proteins. *Curr. Opin. Struct. Biol.* 13, 412–417.
- (33) Mackenzie, K. R. (2006) Folding and stability of  $\alpha$ -helical integral membrane proteins. *Chem. Rev.* 106, 1931–1977.
- (34) Hu, N. J., Iwata, S., Cameron, A. D., and Drew, D. (2011) Crystal structure of a bacterial homologue of the bile acid sodium symporter ASBT. *Nature* 478, 408–411.